JOURNAL OF CATALYSIS 103, 140–150 (1987)

# Simulation of Supported Iridium Catalyst Sintering and Redispersion

RICHARD W. RICE AND CHILING C. CHIEN

*Department of Chemical Engineering, Clemson University, Clemson, South Carolina 29634-0909*

Received April 30, 1986; revised August 5, 1986

During periodic coke-burnoff as well as during normal use, naphtha reforming catalysts may lose activity due to metal sintering. Such deactivation can be offset by *in situ* redispersion treatments. This paper describes a Monte Carlo method-based computer simulation of both phenomena for iridium (or Pt/Ir) supported on chlorinated alumina. The model incorporates both molecular and crystallite migration mechanisms, plus possible vapor phase transport and the concept of "chemical trap" sites. Both sintering and redispersion have been simulated in numerous runs aimed at determining the effect of atmosphere, metal loading, temperature, time, etc., on dispersion. The predictions of the model qualitatively describe experimentally observed behavior. 

## INTRODUCTION

Perhaps the most significant application of supported noble metal catalysts is for reforming low octane naphtha to high octane unleaded gasoline. Such catalysts deactivate during use due to carbonaceous residue (coke) formation, poisoning by feed impurities, e.g., sulfur, heavy metals, etc., and active metal crystallite growth, i.e., sintering. This paper deals with the topic of sintering and with the manner by which it can be reversed, i.e., redispersion. Sintering can occur in both reducing and oxidizing atmospheres, but is most rapid in the coke-burnoff regeneration cycle of the process. Restoring a badly sintered catalyst to a highly dispersed, active state can be accomplished by an *in situ* redispersion treatment with a chlorine containing gas mixture.

One of the earliest theoretical/modeling treatments of catalyst sintering was the crystallite migration model of Ruckenstein and Pulvermacher (*1*). This was followed by the molecular migration model of Wanke and Flynn (*2, 3*) and extensions of it (*4, 5*). Most experimental research on sintering has focused on Pt (*6–16*) supported on $Al_2O_3$ or $SiO_2$, but Ir has been examined in a few cases (*14–18*). Platinum–iridium bimetallic reforming catalysts, while not as widely employed commercially as Pt or Pt/Re, are of interest because of their high activity. At high temperatures in the presence of $O_2$, the Ir component of Pt/Ir forms a stable bulk oxide, $IrO_2$, unlike Pt which primarily forms only a surface oxide. This $IrO_2$ does not interact as strongly with the support as Pt oxide and because of its higher mobility sinters more rapidly than Pt (*15, 16*). Compared to sintering, redispersion has been rarely discussed (*18–22*) in the open literature and in most such cases only temporary, small extents of redispersion associated with Pt in $O_2$ over a narrow temperature range have been reported. It is known that the surface chloride content of a reforming catalyst has a profound influence on the sintering/redispersion behavior of such catalysts (*23, 24*), but the role played by Cl is not fully understood. Lieske *et al.* (*21*) in studies of $Pt/Al_2O_3$ in $O_2$ and $O_2/Cl_2$ hypothesized that redispersion requires reaction of surface Cl with $PtO_2$ to form a mobile oxychloride which subsequently becomes trapped at an energetically favorable site. Associating such sites with Cl is suggested by the work of McVicker *et al.* (*18*) in which "chemical trap



0021-9517/87 $3.00

sites" are proposed to account for Ir redispersion in $O_2$ for Group IIA oxide-impregnated $Ir/Al_2O_3$ catalysts. Straguzzi *et al.* (*22*) pictured trap sites on $Pt/Al_2O_3$ in an oxidizing atmosphere as being exposed Al atoms with neighboring OH groups replaced by Cl. A similar situation would be expected for $Ir/Al_2O_3$, but unlike Pt, substantial Ir redispersion requires prereduction with $H_2$ followed by exposure to $Cl_2$ rather than $O_2$ (*24*).

Sintering and redispersion are complex phenomena, depending on a large number of variables; and, although the complete set of potential variables were not examined in this present work, a sufficiently large number of variables were treated to favor using a computer simulation based on Monte Carlo methods as opposed to more conventional modeling. This was accomplished by breaking a complex overall process down into separate (but interacting) simpler phenomena for which the Monte Carlo method is better suited. This technique has been applied to model $Pt/Al_2O_3$ sintering and, to a minor extent, redispersion by Handa and Matthews (*13*). The work here contains some basic features drawn from their paper, but deals with a different system, involves a greatly expanded number of mechanisms and variables, and is, to the authors' knowledge, the first attempt to comprehensively model redispersion. It should further be noted that because the models were developed specifically for $Ir/Al_2O_3$, clearly their application to other metals and/or supports would, at the minimum, require changes in numerous parameter values and might involve more substantial, qualitative changes. For reasonably closely related systems, such as $Ir/SiO_2$ or $Pt/Al_2O_3$, it is likely that the general outline of the models with only modest alteration might be adequate, while for $Ir/TiO_2$, $Ni/SiO_2$, etc., much more might be involved.

## MODEL DEVELOPMENT AND DESCRIPTION

The catalyst simulated was $Ir/Al_2O_3$, but experimental results imply that the behavior of Ir in a $Pt–Ir/Al_2O_3$ catalyst is essentially the same (*25*). An outline of the major features of the sintering model will be presented first, then relevant differences between the sintering and redispersion models will be briefly discussed. Details of both models can be found elsewhere (*26*). The surface of a support is simulated as a square region of a two-dimensional coordinate system in computer memory. Onto this plane are randomly placed particles containing Ir atoms if a hydrogen atmosphere is assumed, $IrO_2$ molecules if an $O_2$ atmosphere is assumed, or iridium chloride molecules if a redispersing ($Cl_2$) atmosphere is assumed. The number of Ir atoms involved is dictated by the assumed metal loading and their initial grouping into what will be termed clusters (particles containing $\leqq 13$ molecules) and crystallites (particles of $\geqq 14$ molecules) is determined by the desired initial fractional exposure (dispersion) and particle size distribution. Throughout a simulation the number of molecules associated with each particle, plus the diameter and coordinates of the center of each hemispherical particle are stored in arrays and updated during each "time step." A time step is a term which is later linearly related to real time and consists of a sequence of separate events which are resolved using probability equations and random numbers, thus this is termed a stochastic or Monte Carlo simulation (*27*). By many repetitions of these discrete but serially connected time steps one can obtain sintering or redispersion histories. The events simulated are (1) dissociation, i.e., detachment of a molecule from a particle, (2) surface diffusion of both parent and detached particles, (3) collision and possible coalescence, and (4) in an $O_2$ atmosphere, vapor transport of a molecule (*15, 25, 28*).

During a given time step each particle is tested for detachment of one molecule via dissociation by the use of a computer-generated random number, $R_n$, with a value from 0 to 1 along with Eq. 1,

$$F = \left(1 - \frac{N_m}{N}\right) \cdot \Delta SCN_n \cdot \exp\left[\frac{E_d}{R}\left[\frac{1}{T_0} - \frac{1}{T}\right]\right]. \quad (1)$$

Here $F$ represents the fractional probability that dissociation will occur, $N_m$ is the number of metal atoms associated with mobile clusters, $N$ is the total number of metal atoms in the system, $\Delta SCN_n$ is a factor defined later, $E_d$ is an activation energy for dissociation, $R$ is the ideal gas constant, $T$ is the system's temperature in °K, and $T_0$ is a reference temperature chosen as the maximum temperature at which no appreciable sintering occurs (= 673°K in $O_2$). The $\Delta SCN_n$ term attempts to account for a size dependence of the parent crystallite by relating dissociation probability to the departure of the average surface coordination number (SCN) of the crystal from the maximum value of 8 for an infinitely large face-centered cubic crystallite. As shown in Eq. (2), this value is divided by a similar quantity (8-SCN*) for the minimum sized complete fcc crystallite (14 molecules) to yield a value for $\Delta SCN_n$ between 0 and 1,

$$\Delta SCN_n = \frac{8\text{-SCN}}{8\text{-SCN}^*}, \quad (2)$$

where SCN* $\approx$ 5.1. Given that SCN = 3 for corner atoms, 5 for edge atoms, and 8 for face atoms, $\Delta SCN_n$ increases with decreasing crystallite size and is set equal to unity for clusters (*13, 26*). This concept is similar to the increase in vapor pressure with decreasing radius of curvature predicted by the Kelvin equation. The $(1 - N_m/N)$ term was inserted to provide a type of equilibrium dampening as the population of mobile clusters increases. This is relatively unimportant for sintering but plays a major role in redispersion. An equation similar to Eq. (1) involving $\Delta SCN_n$, but without the first term and with a different activation energy, $E_a$, and a constant factor, $A_v$, is used to obtain the evaporation probability, $\phi$, for sintering in $O_2$. If the test random number, $R_n$, is less than or equal to the probability value, the event occurs, e.g., if $R_n \leqq F$, a molecule at a randomly selected point on the edge of the circular projection of the crystallite on the surface is allowed to move via surface diffusion a distance, $L_s$, in a randomly determined direction. Similarly, the parent particle is tested for movement. Note that this distance, $L_s$, is intended not as a single "hop" value but as the net distance traversed during the real time interval corresponding to one time step. The distance, $L_s$, in nanometers, is given by

$$L_s = (\mu + \sigma I) \cdot N_T^{-1/2} \quad (3)$$

where $\mu$ and $\sigma$ represent the mean and standard deviation of a normal distribution of step lengths, $I$ is a normal random variable between $-1$ and 1, and $N_T$ is the number of atoms in the moving particle. This last term accounts for a decrease in mobility with increasing size and both $\mu$ and $\sigma$ are temperature dependent with an activation energy of $E_s$, e.g.,

$$\mu = \mu_0 \cdot \exp\left[\frac{E_s}{R}\left(\frac{1}{T_0} - \frac{1}{T}\right)\right]. \quad (4)$$

This introduces, indirectly, an expected increase in actual "hop" frequency during a time step when $T$ increases. For the 673–873°K range, values of $\mu$ and $\sigma$ were chosen to give single molecule $L_s$ values of 3–9 nm, the pore size range containing most of the area for a reforming catalyst. Each time a particle moves, a check for collision with another particle is made. If the projected path indicates collision, a test for coalescence is made using a test random number and the following equation for capture probability, $S_F$,

$$S_F = 1 - \Delta SCN_n \cdot \exp\left[\left(\frac{E_n}{R}\right)\left[\frac{1}{T} - \frac{1}{T_0}\right]\right], \quad (5)$$

where $E_n$ is the activation energy for capture. In the case of evaporation an $IrO_3(g)$ molecule is assumed to move fast enough to

have a chance to readsorb at any spot on the surface. The overall dispersion, SD, is calculated after each time step by summing the total number of surface metal atoms and dividing by the total number of metal atoms. The number of surface atoms for a given particle is determined using approximate equations (*29*) for fcc cubes adjusted to account for both the assumed hemispherical shape and the "bottom" atoms contacting the support. Likewise, the projected diameter of each simulated particle is obtained by using estimated molecular sizes for Ir, $IrO_2$, $IrCl_3$, etc., in equations from this source. Because increasing the chloride concentration retards sintering, a "trap" feature can be used in the model. To simulate cases in which the surface Cl level is appreciably higher than some threshold value, possibly that corresponding to the Cl in the $H_2IrCl_6$ typically used to make such catalysts, a number of fixed trap sites (0.5 nm in diameter) are randomly placed. A migrating particle encountering such a trap becomes immobile, but may still gain or lose molecules.

The redispersion model is structurally similar to the sintering model, but with the following important differences: (1) $IrCl_3$ is the mobile species, (2) no vapor transport is assumed, (3) the activation energy values, $E_d$, $E_s$, and $E_n$, are different, and (4) for multicycle $Cl_2$ treatments, clusters are assumed to become immobilized after intercycle $H_2$ reduction. Redispersion, although the opposite of sintering, involves essentially the same mechanistic features, e.g., detachment, transport, coalescence, but with radically different relative rates for these competing effects. The effect of the atmosphere, e.g., $Cl_2$ versus $O_2$, and for that matter, the effect of surface species and/or support identity can, at present, only be introduced through changes in key parameters and assumptions as indicated above. Both models are believed to be plausible, but are, of necessity, relatively empirical, requiring either parameter estimation or fitting to data.

## RESULTS AND DISCUSSION

In developing the two models many runs were made to determine the relative importance of the separate features and to select reasonable values for parameters. This section will describe the findings of a sampling of these runs. The results are qualitative predictions of general sintering and redispersion trends for different conditions. Finally, comparisons of simulation results with experimental data are made.

### *Sintering*

From the beginning it was recognized that the size of the system for a given loading would influence long-term sintering results because the dispersion value for a single crystallite containing all of the metal atoms represents a lower bound. This was confirmed by a series of runs simulating a 1 wt% $Ir/Al_2O_3$ catalyst in $O_2$ at 773°K for five different system side lengths ranging from 50 to 250 nm. For all but the 50-nm system the dispersion versus time profiles (histories) were smooth, qualitatively similar curves, thus it was felt that a 100-nm square would be adequate for development runs. Unless otherwise specified, it may be assumed that subsequent sintering runs were made on a "base case" $Ir/Al_2O_3$ catalyst with the following features and simulation parameters: 1 wt% Ir, 1 wt% Cl, 200 $m^2/g$ support, approximately normal initial crystallite size distribution, 100 nm side length, 1566 Ir atoms, $O_2$ atmosphere, $E_d = 0$, $E_a$, $E_s$, and $E_n$ = 16, 10, and 8 kcal/mole, respectively, $A_v = 0.125$, $\mu_0 = 1.5$ nm, $\sigma_0 = 0.15$ nm, $T_0 = 673$°K, and $T = 773$°K. The step size reference parameters $\mu_0$ and $\sigma_0$ chosen were the largest ones which still gave negligible sintering after 2000 time steps at 673°K. For sintering in $H_2$, $A_v = 0$ (due to the negligible vapor pressure of Ir at any reasonable $T$), $E_d$, $E_s$, and $E_n$ = 0, 1.3, and 4 kcal/mole, respectively, $\mu_0 = 2$ nm, $\sigma_0 = 0.2$ nm, and $T_0 = 773$°K. To determine whether the "seed value" used in the random number generation subroutine had an

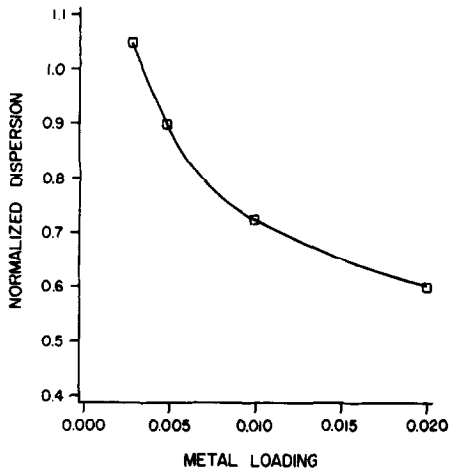


FIG. 1. Effect of metal loading (mass fraction) on simulated $Ir/Al_2O_3$ sintering behavior in $O_2$ at 773°K after 2000 time steps for ISD = 0.46.

appreciable effect on the overall simulation, a series of otherwise identical runs were made using different seed values. The results confirmed that only minor variations occurred. Nevertheless, except for the large system simulations involved in comparing model predictions with experimental data, results shown are the average of three such runs involving different seeds. The effect of specific parameters will now be examined.

*Initial particle size distribution.* Three cases, all involving 1 wt% Ir and an initial dispersion of 0.63, but with different initial particle size distributions were simulated for 2000 time steps at 773°K. The bimodal case, involving 11 $IrO_2$ particles of 2.1 nm diameter and 85 particles of 1.15 nm diameter, showed a slightly greater sintering rate (final dispersion = 0.33) than a Gaussian distribution case with a mean diameter of 1.4 nm. The unimodal case (1.4 nm) displayed the lowest sintering rate, with a final dispersion of 0.37. These results can be explained in terms of the several larger crystallites in the bimodal case serving as more efficient "net acceptors" for migrating particles due to a lower evaporation rate and a higher capture probability.

*Variation of particle size distribution with time.* Particle size distribution was periodically examined during both sintering and redispersion simulations. In sintering cases it was noted that the distribution broadened very early around the initial mean and later, typically after only 500 to 1000 time steps, developed peaks at sizes distinctly larger and smaller than the starting size range.

*Metal loading.* Figure 1 shows, as expected, that increasing the metal loading leads to an increase in collision frequency and thus in sintering rate. The quantity shown, normalized dispersion, is defined as dispersion (SD) at time, $t$, divided by initial dispersion (ISD = 0.46 in these cases). The value of 1.05 for the lowest loading case reflects a small redispersion transient inherent in the model for low-loaded catalysts in the early stages of sintering when dissociation/evaporation is temporarily more frequent than capture. This may have a basis in fact (*16, 17*) for short exposure to $O_2$.

*Initial dispersion.* Table 1 shows that fitting the results of 773°K sintering simulations for 1 wt% Ir unimodal catalysts with three different initial dispersions to a power law equation,

$$\frac{-d(\mathrm{SD})}{dt} = k(\mathrm{SD})^n \qquad (6)$$

resulted in an increase in the apparent order, $n$, with increasing initial average particle size, in agreement with the molecular migration model (*2*). After 3000 time steps in $O_2$ all three cases were approaching SD $\approx$ 0.30.

TABLE 1

The Effect of Initial Dispersion on Simulated Sintering Behavior (150-nm square system)

| Case | Diameter of $IrO_2$ crystallite (nm) | Initial number of crystallites | Initial dispersion ISD | Power law order, $n$ |
|---|---|---|---|---|
| 1 | 1.4 | 189 | 0.62 | 3.2 |
| 2 | 2.8 | 20 | 0.43 | 4.2 |
| 3 | 4.2 | 6 | 0.34 | 6.9 |

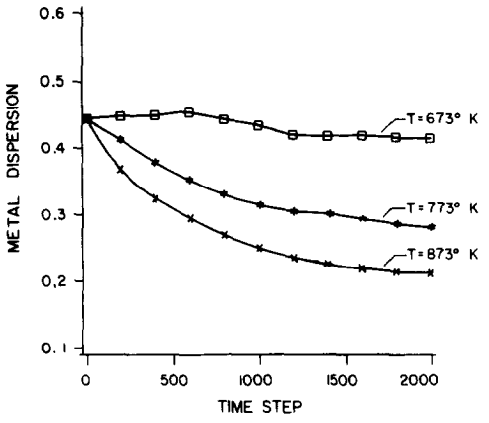


FIG. 2. Effect of temperature on simulated sintering behavior in $O_2$ for a normally distributed 1 wt% Ir/$Al_2O_3$.

*Temperature.* In Fig. 2 it can be seen that after 2000 time steps at 673°K in $O_2$ a base case catalyst had a negligible decrease in dispersion from an initial value of 0.46, but lost 39 and 52% of its original area at 773 and 873°K, respectively.

*Chloride.* As indicated earlier, any Cl in excess of some threshold value, possibly that associated with the $H_2IrCl_6$ typically used in preparing an Ir/$Al_2O_3$ catalyst, was expressed in the model as a number of trap sites. A series of runs was made to determine the effect of trap density, i.e., number of traps per unit support area (1/nm$^2$), on dispersion at three different temperatures for a simulated 1 wt% Ir/$Al_2O_3$ catalyst with an initial dispersion of 0.46. Figure 3 shows that increasing trap density considerably reduces the sintering rate and can seemingly enable redispersion to occur in $O_2$ at very high Cl levels. This latter prediction can only be considered highly speculative in the absence of experimental results for such conditions and considering that such high trap densities may not be achievable in $O_2$.

*Activation energies.* Except for an estimate of 16 kcal/mole for the activation energy for evaporation of Ir in an $O_2$ atmosphere (*30*), no experimental information on the various activation energies employed in the models could be found. Thus, a combination of educated guessing and trial and error was used to set these values. Figure 4 shows the sensitivity of sintering simulation results to the value of $E_s$, the diffusional activation energy.

*Effect of atmosphere and comparison with experimental data.* Comparisons were made of the sintering behavior in both $O_2$ and $H_2$ atmospheres for an actual experimental 1 wt% Ir/$Al_2O_3$ catalyst (*16*) and a

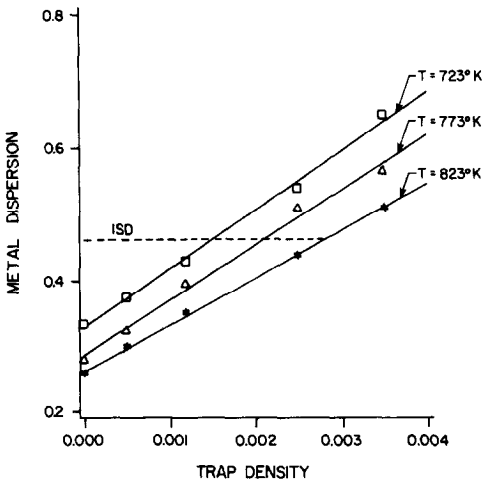


FIG. 3. Effect of chloride-related trap density on simulated sintering behavior in $O_2$ for 1 wt% Ir/$Al_2O_3$ (ISD = 0.46) after 2000 time steps.

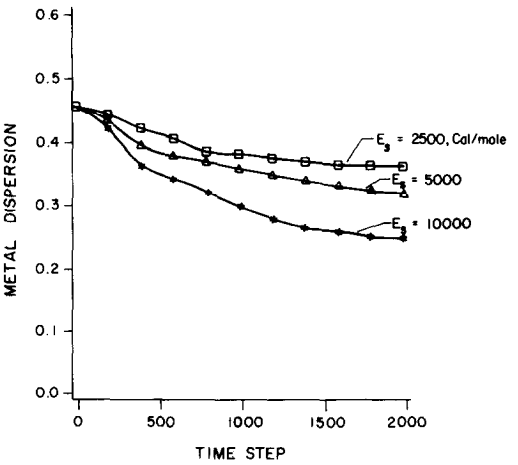


FIG. 4. Effect of the activation energy of diffusion on the sintering behavior in $O_2$ for 1 wt% Ir/$Al_2O_3$ at 773°K.

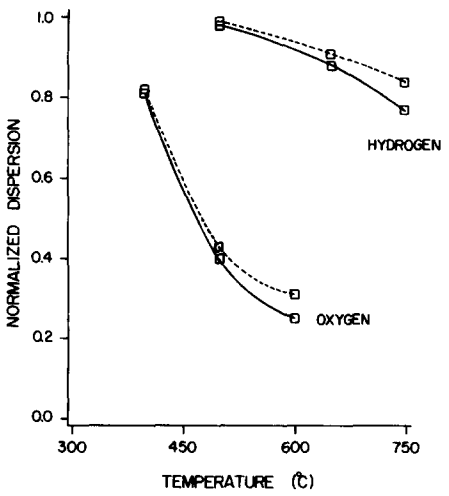


FIG. 5. Comparison of simulation results and experimental data (Graham and Wanke) for a 1 wt% $Ir/Al_2O_3$ catalyst with ISD = 0.46 in $H_2$ and $O_2$ atmospheres. The dashed curves represent simulation results after 3000 time steps; the solid curves depict data for 1 hr of real time.

simulated, normally distributed catalyst having the same properties, i.e., 96 $m^2/g$ support area and an initial dispersion of 0.46. In these runs a large system, 250 nm side length, with roughly 10,000 Ir atoms was used. Based on experimental results for 1 hr of sintering, a rough "conversion factor" of 3000 time steps being equivalent to 1 hr of real time was found to be suitable. This equivalence was used in preparing Fig. 5, which shows that the sintering model matches the experimental data well for both $H_2$ and $O_2$ atmospheres over a broad temperature range. The fact that the model slightly underpredicts sintering at the highest temperatures studied may indicate a need for additional refinements in a $H_2$ atmosphere, but for the $O_2$ case probably reflects the aforementioned problem of the limited system size dampening the sintering rate at very low dispersion values.

*Redispersion*

The redispersion model base case simulation properties were: $A_v = 0$, $E_d$, $E_s$, and $E_n = 10$, 5, and 0.5 kcal/mole, respectively; $T_0 = 773°K$, $\mu_0 = 2$ nm, and $\sigma_0 = 0.2$ nm. A diffusing $IrCl_3$ species in a $Cl_2$ atmosphere was assumed and a somewhat larger system (150 nm side length, 3524 Ir atoms/wt% Ir) was used for the development runs. Except for a few cases specified later, a unimodal initial particle size distribution was used. It was found that this gave essentially the same results as the normal distribution for initially badly sintered catalysts. The redispersion model as initially developed did not involve the use of trap sites, thus, unless otherwise stated, this feature was absent. However, it was found necessary to invoke traps in order to achieve simulated redispersion of highly agglommerated $Ir/Al_2O_3$ catalysts, e.g., those with an average $IrO_2$ crystallite size $\geq 6$ nm. Physically, the trap site density may again be pictured as a measure of surface Cl concentration in excess of some "normal" or reference value; but in this case, based on what the literature (*24*) indicates as the minimum catalyst Cl/metal ratio for redispersion and the fact that the surface is in contact with $Cl_2(g)$, a reasonable assumption is that the reference (no trap) catalyst Cl mass fraction is roughly 1.5 to 2 times the metal mass fraction. In actual redispersion practice the "excess" equilibrium Cl concentration often varies from 0 to 1.5 wt% depending on the $H_2O/Cl_2$ ratio used in the treat gas. With this as a preface, the following parameters will now be discussed.

*Initial particle size distribution.* Redispersion simulations were made on three $Ir/Al_2O_3$ catalysts at 773°K, all having the same initial dispersion (0.33), but with the following different Ir particle size distributions and diameters: (1) unimodal (3.0 nm), (2) bimodal (3.4 and 1.0 nm), and (3) a narrow normal distribution with a mean of 3.0 nm and a standard deviation of 0.12 nm. After 400 time steps the dispersion values lined out at 0.43, 0.33, and 0.40, respectively. The lack of redispersion for the no-trap, bimodal case points up the fact that, as suggested in the literature (*4*), there may be a critical crystallite size above which redispersion is extremely slow. In the model

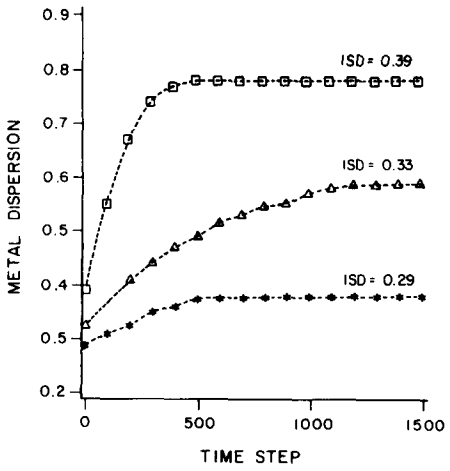


FIG. 6. Effect of initial dispersion on redispersion behavior for 1 wt% unimodal $Ir/Al_2O_3$ in $Cl_2$ at 773°K.

this results because a 3.4-nm Ir crystallite when converted to an $IrCl_3$ crystallite is in the low asymptotic region of the dissociation probability curve yet has a high capture probability.

*Metal loading.* Four $Ir/Al_2O_3$ catalysts with the same initial dispersion (0.29), but different Ir mass fractions (0.003, 0.005, 0.01, and 0.02) were subjected to a simulated $Cl_2$ redispersion at 773°K. Dispersion lined out after 500 to 1500 time steps and the respective values at 2000 time steps were 0.48, 0.42, 0.37, and 0.33. Comparing the 66% redispersion of the lowest loaded catalyst with the 14% value for the highest (0.02) loaded catalyst confirmed the expected greater difficulty of redispersing Ir on a more crowded surface where recapture of migrating $IrCl_3$ competes effectively with dissociation.

*Initial dispersion.* Figure 6 shows the dramatic effect that seemingly small differences in initial dispersion (ISD) have on redispersion behavior for 1 wt% $Ir/Al_2O_3$ catalysts having the following ISD and Ir crystallite diameter values: (1) 0.39 (2.3 nm), (2) 0.33 (3.0 nm), and (3) 0.29 (3.4 nm). As implied earlier, there appears to be a threshold Ir crystal size in the range 3.2–3.4 nm, above which substantial redispersion requires either alternate, multicycle $H_2/Cl_2$ treats or the establishment of an appreciable excess Cl level expressed as a non-zero trap density in the model.

*Temperature.* Redispersion of a 1 wt% $Ir/Al_2O_3$ catalyst with an initial dispersion of 0.33 was simulated at three different temperatures. Figure 7 shows that both the rate and ultimate extent of redispersion were very sensitive to temperature, with dispersion increasing by only 18% at 723°K, but by 133% at 823°K. This reflects the fact that, as temperature increased, the increased dissociation rate more than offset the increased migration speed and coalescence probability.

*Chloride.* The nature of trap sites and their association in the redispersion model with what may be thought of as surface Cl in excess of some critical $Cl/IrCl_3$ ratio has been introduced earlier, thus the discussion here will be strictly on the effect of this model parameter. Simulation runs were made on a 2 wt% $Ir/Al_2O_3$ catalyst in $Cl_2$ at 773°K assuming a number of traps ranging from 0 to 300, corresponding to a trap density range of 0 to 0.0133 traps/nm$^2$. Dispersion rose from an initial value of 0.33 to a steady state value within 1000–1500 time steps. Figure 8 shows that the normalized final dispersion, SD/ISD, after 2000 time

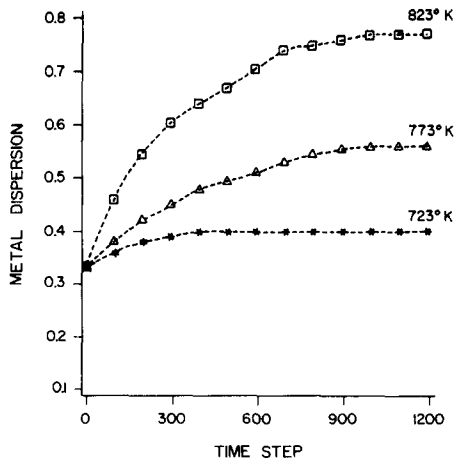


FIG. 7. Effect of temperature on redispersion behavior for 1 wt% $Ir/Al_2O_3$ in $Cl_2$.

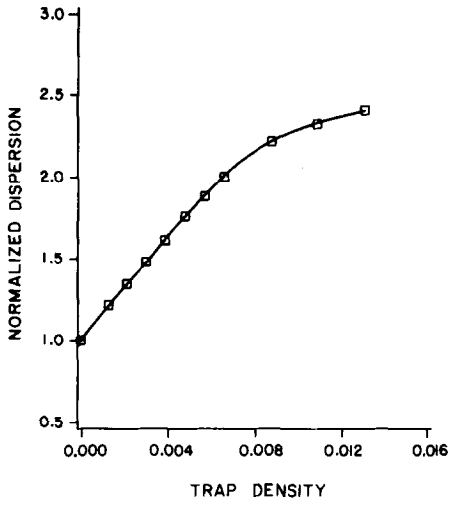


FIG. 8. Normalized dispersion versus trap density for 2 wt% $Ir/Al_2O_3$ in $Cl_2$ at 773°K after 2000 time steps.

steps increased nearly linearly with increasing trap density up to a trap density of 0.008, then appeared to be approaching a limiting value of roughly 2.5. This asymptotic dispersion value of roughly 0.825 is the value associated with clusters of 5–10 Ir atoms (0.6 to 0.9 nm), which, although not complete atomic dispersion, is essentially as high as the model predicts, given its assumptions about particle geometry.

*Multicycle $H_2/Cl_2$ treatments.* Yates (*31*) has reported that two consecutive 3-hr $Cl_2$ treatments with an intercycle $H_2$ reduction resulted in considerably better redispersion of a severely agglomerated $Pt–Ir/Al_2O_3$ catalyst than did a single 6-hr $Cl_2$ treat. A similar advantage for multicycle relative to monocycle treating for a fixed total time has been reported by Fung and Rice (*24*). The simulation model developed here assumes that during the intercycle $H_2$ reduction all moving $IrCl_3$ clusters are converted to immobile Ir clusters, perhaps via strong Cl linkages, and remain immobile during any further $Cl_2$ treatment. This makes subsequent treats more effective because (1) crystallites have little chance of capturing such clusters and (2) the effective dissociation probability of crystallites is increased due to the decrease in the population of moving clusters. Figure 9 shows a comparison of a two-cycle $Cl_2/H_2$ simulation with a conventional one-cycle case at 773°K for a 1 wt% $Ir/Al_2O_3$ catalyst (no traps) with ISD = 0.29. The second cycle was clearly very effective, as has been observed in actual practice.

*Comparison with experimental data.* A large system with a 250-nm side length was used to determine how well the model could simulate some experimental results (*31*) for the redispersion of a 1 wt% $Ir/Al_2O_3$ catalyst with an initial average Ir crystallite diameter of 5.0 nm (ISD = 0.22) at 773°K in a $Cl_2/O_2$ atmosphere. Except for a somewhat higher $E_d$ value (15 kcal/mole), the standard redispersion model parameter values given earlier were used along with a trap density of 0.0048 traps/nm$^2$ in generating the dispersion versus time profile shown in Fig. 10. Only the initial and final (after 3 hr) experimental dispersion values were known, thus the dotted line connecting these two points is merely for reference and is unrealistic at high dispersion where the approach to nearly complete dispersion dampens the redispersion rate, as the simu-

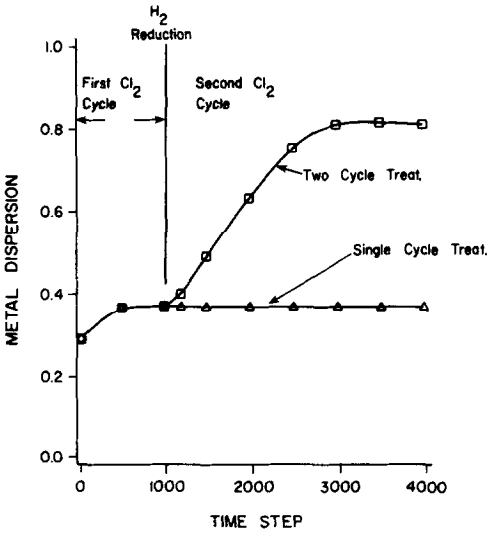


FIG. 9. Comparison of a simulated alternate $H_2/Cl_2$ two-cycle treatment with a single $Cl_2$ treatment for 1 wt% $Ir/Al_2O_3$ at 773°K.

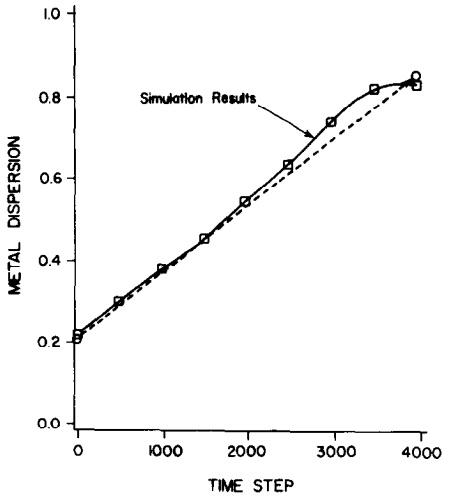


FIG. 10. Comparison of simulated redispersion results with experimental data (Yates) for 1 wt% Ir/$Al_2O_3$ at 773°K. The circles represent initial and final experimental values; the dotted line merely connects these two points.

lation data show. This comparison allows one to make a rough guess as to the real time equivalent of one time step. In this case one time step appears to correspond to 2.3 real seconds, roughly twice the value found for sintering. A higher value, 3.6 s/time step, was found when a redispersion simulation was matched with a second set of experimental data (*31*) for a 1 wt% Ir/$Al_2O_3$ catalyst with ISD = 0.20. Experimentally, after 3 hr of $Cl_2$ treating at 773°K, the dispersion had increased to 0.40. This same result was obtained from the simulation for a treatment of 3000 time steps assuming a trap density of 0.004 and an $E_s$ value of 8 kcal/mole.

Finally, a third comparison of the simulation predictions with experimental data was made using a case (*24*) involving a 53-min, 797°K, $Cl_2/H_2O$ treatment of a 0.3% Ir, 0.3% Pt on alumina catalyst following an HCl pretreatment. In the experiment the catalyst had ISD = 0.32 and after the redispersion treatment dispersion was 0.87. It was decided to determine the sensitivity of the real time/time step ratio to a change in the $E_d$ value. By lowering $E_d$ to the base case value of 10 kcal/mole while holding everything else constant, including the trap density value of 0.0048, a very good match between experiment and simulation was obtained for a time ratio of 2.6 s/time step. On the other hand, when this same simulation was run using the $E_d$ value of 15 kcal/mole used to simulate Yates' data, the time ratio value increased to 3.9 s/time step. Realistically, considering the wide variations under experimental treatment conditions ($Cl_2/O_2$ versus $Cl_2/H_2O$, HCl pretreatment or not, etc.) and in catalyst properties (1 wt% Ir versus 0.3% Ir/0.3% Pt, ISD = 0.20 to 0.32, etc.), it is perhaps remarkable that there is not a greater variation in apparent time ratio values. For the long duration, high final dispersion case of Fig. 10, it is possible that the experimental catalyst's dispersion had lined out before the treatment time given, and, if so, a time ratio value closer to those for the other experimental cases would have resulted. In the absence of controlled experimentation made for the sole purpose of acquiring detailed dispersion versus time profiles as opposed to merely initial/final values, it can only be said that one time step of the current redispersion model corresponds to roughly 3 s of real time. Likewise, without information concerning post-treatment catalyst Cl loadings, which was not available for the experimental cases used, a quantitative correspondence between trap density values and actual excess Cl values cannot be made at present.

## REFERENCES

1. Ruckenstein, E., and Pulvermacher, B., *AIChE J.* **19,** 356 (1973).
2. Flynn, P. C., and Wanke, S. E., *J. Catal.* **34,** 390 (1974).
3. Flynn, P. C., and Wanke, S. E., *J. Catal.* **34,** 400 (1974).
4. Ruckenstein, E., and Dadyburjor, D. R., *J. Catal.* **48,** 73 (1977).
5. Lee, H. H., *J. Catal.* **63,** 129 (1980).
6. Dautzenberg, F. M., and Wolters, H. B. M., *J. Catal.* **51,** 26 (1978).
7. Hassan, S. A., Khalil, F. H., and El-Gamal, F. G., *J. Catal.* **44,** 5 (1976).
8. Yao, H. C., Sieg, M., and Plummer, H. K., Jr., *J. Catal.* **59,** 365 (1979).

9. Lietz, G., Lieske, H., Spindler, H., Hanke, W., and Volter, J., *J. Catal.* **81,** 17 (1983).
10. Harris, P. J. F., *J. Catal.* **97,** 527 (1986).
11. Flynn, P. C., and Wanke, S. E., *J. Catal.* **37,** 432 (1975).
12. Chu, Y. F., and Ruckenstein, E., *J. Catal.* **55,** 281 (1978).
13. Handa, P. K., and Matthews, J. C., *AIChE J.* **29,** 717 (1983).
14. Wanke, S. E., *Mater. Sci. Res.* **16,** 223 (1984).
15. Fiedorow, R. M., Chahar, B. S., and Wanke, S. E., *J. Catal.* **51,** 193 (1978).
16. Graham, A. G., and Wanke, S. E., *J. Catal.* **68,** 1 (1981).
17. Wang, T., and Schmidt, L. D., *J. Catal.* **66,** 301 (1980).
18. McVicker, G. B., Garten, R. L., and Baker, R. T. K., *J. Catal.* **54,** 129 (1978).
19. Foger, K., and Jaeger, H., *J. Catal.* **92,** 64 (1985).
20. Lee, T. J., and Kim, Y. G., *J. Catal.* **90,** 279 (1984).
21. Lieske, H., Lietz, G., Spindler, H., and Volter, J., *J. Catal.* **81,** 8 (1983).
22. Straguzzi, G. I., Aduriz, H. R., and Gigola, C. E., *J. Catal.* **66,** 171 (1980).
23. Bishara, A., Murad, K. M., Stanislaus, A., Ismail, M., and Hussain, S. S., *Appl. Catal.* **7,** 351 (1983).
24. Fung, S. C., and Rice, R. W., U.S. Patent No. 4447551 (1984).
25. Sinfelt, J. H., and Via, G. H., *J. Catal.* **56,** 1 (1979).
26. Chien, C. C., Masters thesis. Clemson University, 1985.
27. Rubinstein, R. Y., "Simulation and the Monte Carlo Method." Wiley, New York, 1981.
28. Cordfunke, E. H. P., and Meyer, G., *Rec. Trav. Chem.* **81,** 670 (1962).
29. Hardeveld, R. V., and Hartog, F., *Surf. Sci.* **15,** 189 (1969).
30. Krier, C. A., and Jaffee, R. I., *Less-Common Met.* **5,** 411 (1963).
31. Yates, D. J. C., U.S. Patent No. 3981823 (1976).